



OPEN

Exploring dihydropyrimidone derivatives as modulators of carbohydrate catabolic enzyme to mitigate diabetes

Syed Parween Ali¹, Farheen Mansoor², Shaymaa Fadhel Abbas Albaayit³✉, Farman Ali⁴, Aayed A. Dera¹, Muhammad Shahbaz^{5,6}, Jawad Ullah⁷, Hailah M. Almohaimeed⁸, Reem M. Gahtani¹, Ahmed M. Abdulfattah^{9,10}, Fahad M. Alshabrmi¹¹, Sarfaraz Alam¹²✉ & Saeed Ullah¹³✉

Diabetes is a prevalent and serious metabolic disorder affecting millions globally, and it poses extensive health risks due to elevated blood glucose levels. One promising approach for managing diabetes is the inhibition of α -glucosidase, an enzyme that plays a crucial role in carbohydrate metabolism. Targeting α -glucosidase can help delay glucose absorption, thus controlling postprandial blood sugar spikes. Dihydropyrimidones, a core structural class present in various biologically active natural compounds, have been recognized for their diverse therapeutic potential, including anti-diabetic properties. In this study, we evaluated a library of previously synthesized 37 Dihydropyrimidone derivatives to assess their potential as α -glucosidase inhibitors. We identified 34 derivatives with significant inhibitory activity, exhibiting IC_{50} values in the range of 5.30–56.72 μ M. Among these, compounds 2, 4–7, 9–11, 13–16, 31, 32, and 33 demonstrated high potency, with IC_{50} values below 20 μ M; the most active compound, 5, achieved an IC_{50} of 5.30 μ M. A detailed kinetic study on compound 5 revealed a competitive inhibition mode with a K_i value of 16.10 ± 0.0075 μ M. Additionally, cytotoxicity assays confirmed that compound 5 is non-toxic to BJ cell lines, underscoring its safety for therapeutic use. The computational studies further supported the inhibitory potential by illustrating key interactions and binding affinities between the Dihydropyrimidone derivatives and the α -glucosidase, highlighting these compounds as promising candidates for diabetes management.

Keywords α -Glucosidase inhibition, Non-cytotoxicity, Dihydropyrimidone, Diabetes therapy, Molecular docking simulation, Kinetics

Diabetes is a well-known global health issue and the most prevalent metabolic illness in both developing and developed nations. By 2030, the WHO projects that there will be 366 million cases, up from 171 million in 2000¹. Type-II diabetes mellitus, which has multiple aetiologies and is caused by chronic hyperglycaemia, insulin resistance, and dyslipidaemia, is frequently linked to metabolic diseases. The primary causes of diabetes mellitus

¹Department of Clinical Laboratory Sciences, College of Applied Medical Sciences, King Khalid University, Abha 62529, Saudi Arabia. ²Dr. Panjwani Center for Molecular Medicine and Drug Research, International Center for Chemical and Biological Sciences, University of Karachi, Karachi 75270, Pakistan. ³Department of Biology, College of Science, University of Baghdad, Baghdad, Iraq. ⁴Department of Chemistry, Federal Urdu University of Arts, Sciences and Technology, Karachi 75300, Pakistan. ⁵Faculty of Chemistry, Jagiellonian University, Gronostajowa 2, Krakow 30–387, Poland. ⁶School of Exact and Natural Sciences, Jagiellonian University, Łojasiewicza 11, Krakow 30–348, Poland. ⁷Department of Chemistry, Hazara University, Mansehra 21120, Pakistan. ⁸Department of Basic Science, College of Medicine, Princess Nourah bint Abdulrahman University, P.O.Box 84428, Riyadh 11671, Saudi Arabia. ⁹Department of Medial Laboratory Sciences, Faculty of Applied Medical Science, King Abdulaziz University, Jeddah 2158, Saudi Arabia. ¹⁰Embryonic Stem Cell Unit, King Fahd Medical Research Center, King Abdulaziz University, Jeddah 21589, Saudi Arabia. ¹¹Department of Medical Laboratories, College of Applied Medical Sciences, Qassim University, Buraydah 51452, Saudi Arabia. ¹²Biotechnology Centre, Silesian University of Technology, Gliwice 44–100, Poland. ¹³Natural and Medical Sciences Research Center, University of Nizwa, P.O. Box 33, PC 616Birkat Al Mauz, Nizwa, Sultanate of Oman. ✉email: shaymaa_albaayit@yahoo.com; malam@polsl.pl; ahmedsaeedkhan872@gmail.com

are excessive hepatic glucose production or glucose intolerance¹. Additionally, it harms the micro-vascular tissues, leading to complex disorders like retinopathy, nephropathy, and neuropathy. Furthermore, one of the causes of atherosclerosis is postprandial hyperglycaemia^{2,3}. Additionally, it contributes to shorter lifespans and produces certain diabetic complications (micro/macrovacular issues such as ischemic heart disease).

Orally administered antidiabetic drugs have been used either alone or in conjunction with insulin to treat hyperglycaemic individuals^{4–7}. To reach a normal sugar level, numerous anti-diabetic medications were produced in the previous ten years. To prevent diabetes consequences such polyuria, polydipsia, polyphagia, recurrent weight loss, poor vision, nausea, and skin infections, such interventions are unable to lower plasma glucose levels and achieve normoglycemia. Due to this, there is an urgent need to create efficient oral medications that can restore normal glucose and insulin levels^{8–11}.

The exo-type glycosidase enzyme α -glucosidase (EC 3.2.1.20), which is found on the brush borders of the small intestine, catalyses the hydrolysis of carbohydrates from the non-reducing end to produce glucose molecules¹². One of the approved therapeutic targets for the development of medications to prevent problems brought on by hyperglycaemia is α -glucosidase¹³. The α -glucosidase inhibitors AGIs have received a lot of attention lately due to their potential clinical applications as antiviral and hyperglycaemia-controlling medications. α -Glucosidase controlled the conversion of polysaccharides to monosaccharides in the colon, which reduced the blood glucose level. Acarbose, voglibose, and miglitol, three commercially available α -glucosidase inhibitory anti-diabetic medications, are claimed to produce several side effects, including diarrhoea, constipation, abdominal pain, nausea or vomiting, dizziness, pneumatosis intestinalis, and flatulence¹⁴. Therefore, safer α -glucosidase inhibitors are required for use as anti-diabetic medications.

The distinctive and varied motif for drug research, agriculture, and industry is heterocycles. Benzothiazoles are fused bicyclic organosulfur compound in which thiazole ring fused with the benzene ring leads to a class of aromatic compounds presenting an ample collection of biological applications endowed with potent antibacterial¹⁵, antiallergic¹⁶, antifungal¹⁷, anticonvulsant¹⁸, anti-inflammatory¹⁹, anti-helminthic²⁰, antitubercular²¹, and anticancer²². In this reference, the benzothiazole skeleton extensively serves as a significant structural motif and part of various medicinally important compounds. Medicinal researchers paid attention towards the pharmacological aptitude of this chemically diverse skeleton when riluzole approved clinically as an anticonvulsant drug²³. A few derivatives of benzothiazoles, including N-(6-substituted-1,3-benzothiazol-2-yl) benzenesulf-namide were found to have promising antidiabetic potential in vivo in a NIDDM (non-insulin-dependent diabetes mellitus) rat model²⁴. The hypoglycemic activities of the structurally similar benzothiazoles have been reported in recent years^{25–27}.

The literature show the pharmaceutical importance of these dihydropyrimidinone derivatives (Fig. 1). Moreover, Natural and synthetic compounds, alongside traditional medicines, play a crucial role in pharmaceutical development by offering diverse bioactive molecules, enhancing drug discovery, and providing valuable insights into new therapies for treating a wide range of diseases^{30–34}. Therefore, we investigated these compounds for their anti-diabetic capability. The characteristics of pyrimidine derivatives may be helpful in the treatment of diabetes. In addition to playing a variety of roles in biological processes, pyrimidine derivative-containing heterocyclic compounds have important chemical and pharmacological significance in the business. Additionally, the use of pyrimidines conjugated with thiazole nuclei has grown in popularity in clinical and medical settings¹⁵. Dihydropyrimidinones (DHPM), heterocyclic derivatives containing a pyrimidine as a cyclic core moiety, have drawn more attention in medicinal chemistry for a long time because it occur as a key scaffold in natural products with significant biological activity³⁵. Moreover, (DHPM) are also reported for their in vitro α -glucosidase and α -amylase activities [1]. Thiazolopyrimidines have become increasingly well-known in recent years due to their excellent performance in pharmaceutical substances as bioavailable CXCR2 antagonists and anti-diabetic medicines, antimicrobial agents, antioxidants, anti-inflammatory agents, antimalarials, and antitubercular activities, antiviral, and anticancer agents^{36–38}. Moreover, dihydropyrimidinone are also reported for their anti-diabetic potential via targeting they carbohydrates catabolic enzyme α -amylase and α -glucosidase²⁸. In this context we design this study to evaluate these compounds against α -glucosidase.

Results and discussion

General chemistry

Three ingredients were used to create the substituted 4-aryl dihydropyrimidinones in a single pot. Urea, methyl acetoacetate, and a variety of aldehydes are combined in a process at 80 to 90 °C with continual stirring. The catalyst is copper nitrate trihydrate (Scheme 1). The process of heating and stirring was continued until the mixture solidified. Thin layer chromatography was used to assess reaction progress (TLC). After the reaction was finished, the solid product was thoroughly cleaned with distilled water before being recrystallized from ethanol to produce the pure products. ¹H-, ¹³C-NMR, EIMS, and HREI-MS were used to characterize the structures of all synthetic compounds²⁴. Moreover, the mechanism of synthesis is described in (Fig. 2).

In vitro biological evaluation

As the dihydropyrimidinone derivatives are already reported for their anti-diabetic and various other medicinal importance, thus we design this study to explore the therapeutic importance of compounds 1–37. Among them except compounds 19–21 all exhibited potent inhibitory capability with IC₅₀ values ranging 5.30–56.72 μ M (Table 1), while comparing with marketed drug acarbose (IC₅₀ = 873.34 \pm 1.67 μ M). Our findings revealed potent inhibitory capability of these new identified inhibitors. We established a detailed structure activity relationship for all compounds to demonstrate the significance of the attached groups (Fig. 3). For instance, compound 1 with the aryl toluene group substituent resulted into potent inhibition against the key catabolic enzyme of carbohydrates, α -glucosidase with IC₅₀ value 31.16 \pm 0.42 μ M as compared to acarbose. Compound 2 with 1-ethoxy-4-methylbenzene group exhibited significant increase in the inhibitory capability against α -glucosidase

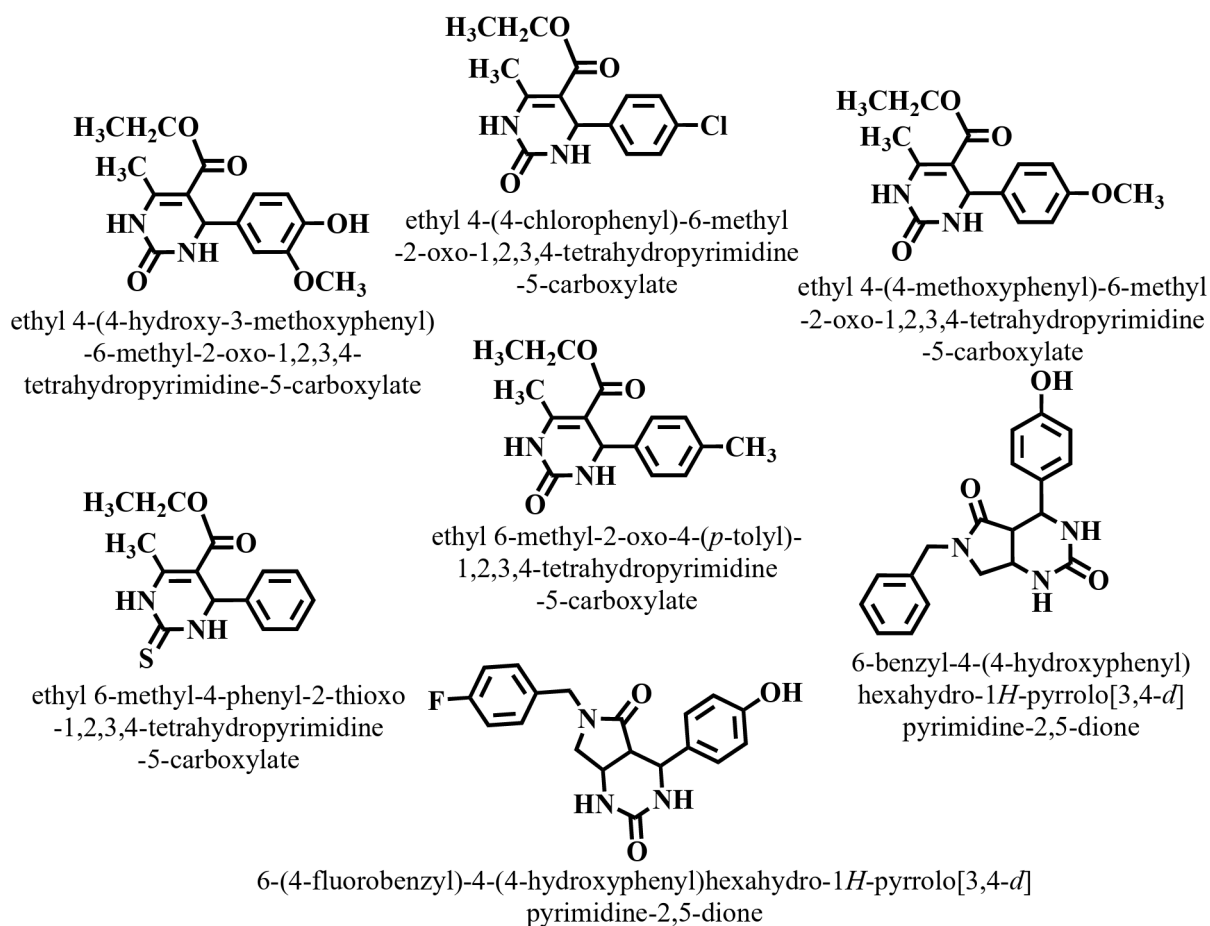
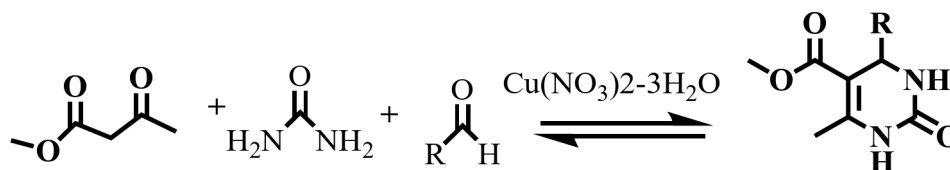


Fig. 1. Some already reported dihydropyrimidinone derivatives^{28,29}.



Scheme 1. Description of the synthesis of one-pot” three component dihydropyrimidinone derivatives 1–37.

($IC_{50} = 9.20 \pm 0.30 \mu M$). While compound 3 with 1-methoxy-4-methylbenzene moiety displayed decline in the inhibitory capability ($IC_{50} = 26.50 \pm 0.63 \mu M$). The effect of methoxy group exhibited an overwhelming inhibition. Like compound 4 with 1-methoxy-2-methylbenzene exhibited potent inhibitory capability ($IC_{50} = 7.34 \pm 0.28 \mu M$).

The inhibitory effect was enhanced in compound 5 with 1,4-dimethoxy-2-methylbenzene ($IC_{50} = 5.30 \pm 0.29 \mu M$), as compared to compound 4. Compound 6 with the substitution of 1,2-dimethoxy-3-methylbenzene exhibited potent inhibitory activity with IC_{50} value $8.42 \pm 0.36 \mu M$. Similarly compound 7 with 1,2-dimethoxy-4-methylbenzene exhibited potent activity against α -glucosidase $11.31 \pm 0.36 \mu M$. In contrast, compound 8 with 2-methoxy-4-methylphenyl acetate exhibited an abrupt decrease in the inhibitory activity with IC_{50} value $37.62 \pm 0.70 \mu M$. Compounds 9 and 10 with 2-fluoro-4-methoxy-1-methylbenzene and 1-fluoro-2-methoxy-4-methylbenzene exhibited almost similar inhibitory effect with IC_{50} values 15.36 ± 0.56 and $17.28 \pm 0.46 \mu M$ respectively. Interestingly, compound 11 with 1-bromo-2,3-dimethoxy-5-methylbenzene also exhibited potent activity against α -glucosidase ($IC_{50} = 13.14 \pm 0.47 \mu M$). On the other hand, compound 12 with 1-(benzyloxy)-2-methoxy-4-methylbenzene displayed decline in the inhibitory activity with IC_{50} value $34.69 \pm 0.72 \mu M$. Compound 13 with 1,2,3-trimethoxy-5-methylbenzene exhibited high potency with IC_{50} value $6.14 \pm 0.27 \mu M$.

The effect of hydroxyl along with halogens was also evaluated for their inhibitory against α -glucosidase. Compounds 14 and 15 with the addition *p*-cresol and *m*-cresol groups resulted into potent activity against α -glucosidase with IC_{50} values 18.26 ± 0.51 and $20.44 \pm 0.38 \mu M$. The inhibitory effect of 2-chloro-4-methylphenol was more favourable and exhibited potent inhibition ($IC_{50} = 14.30 \pm 0.27 \mu M$).

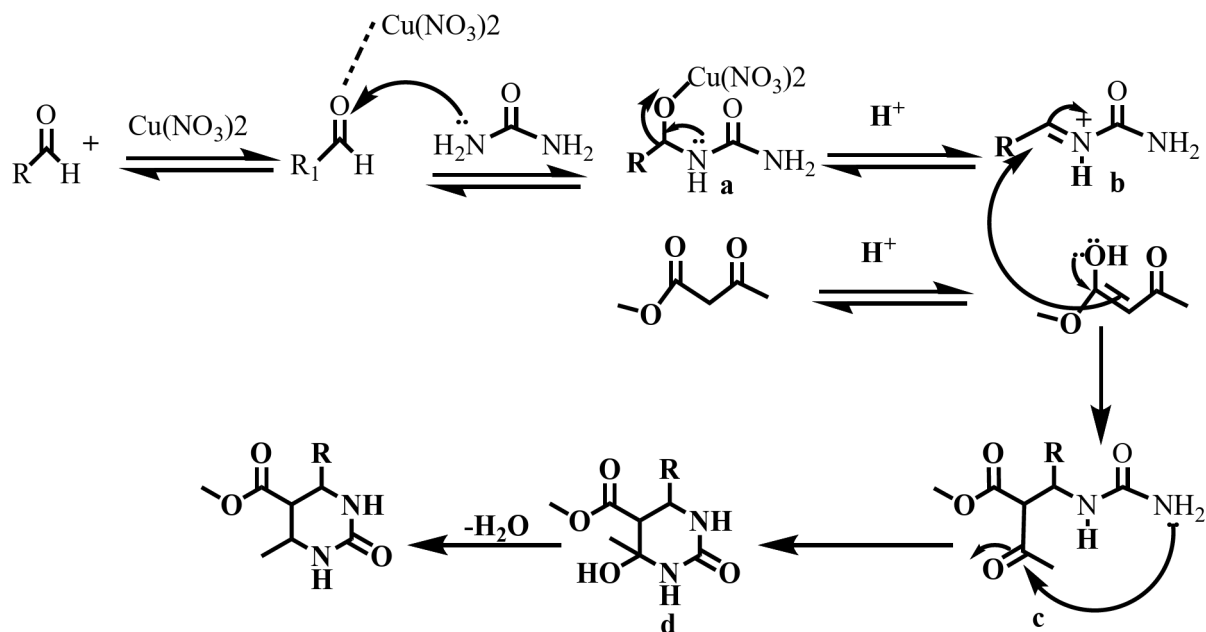


Fig. 2. Description of the synthesis mechanism of dihydropyrimidones.

Compounds **16** and **17** with the substitution of 1-methylnaphthalene and 2-methylnaphthalene groups displayed decrease in their inhibitory activity against α -glucosidase with IC_{50} values 44.64 ± 1.10 and 40.25 ± 0.78 μ M. Compounds **22–24** with the addition of 2-methylfuran, 2,5-dimethylfuran and 3-methylthiophene exhibited very close inhibitory activity against α -glucosidase with IC_{50} values 47.30 ± 1.32 , 50.33 ± 0.23 and 46.25 ± 0.65 μ M. Similarly, compounds **24** and **25** with 2-methylthiophene and 2,5-dimethylthiophene groups displayed almost the same inhibition with IC_{50} values 42.90 ± 0.56 and 39.62 ± 1.11 μ M. The inhibitory effect of halogens exhibited potent inhibitory activity. Compounds **27–29** with 1-chloro-2-methylbenzene, 1,3-dichloro-2-methylbenzene and 1-chloro-4-methylbenzene displayed potent inhibitory activity against α -glucosidase with IC_{50} values 25.40 ± 0.61 , 22.61 ± 0.70 and 27.19 ± 0.46 μ M respectively. The addition of 1-bromo-4-methylbenzene in compound **30** exhibited a slight increase in their inhibitory capability with IC_{50} value 20.17 ± 0.54 μ M. The addition of 1-fluoro-2-methylbenzene in compound **31** further improved their inhibitory effect with IC_{50} value 18.33 ± 0.41 μ M. In contrary, the addition of 1-methyl-4-(trifluoromethyl) benzene in compound **32** resulted decrease in their inhibitory capability with IC_{50} value 26.10 ± 0.56 μ M. In compound **33** the addition of 1-methyl-4-nitrobenzene displayed potent inhibitory capability with IC_{50} value 16.10 ± 0.35 μ M. The inhibitory effect of p-cymene in compound **34** displayed decline in the α -glucosidase inhibition with IC_{50} value 53.19 ± 1.42 μ M. Compound **35** with the addition of N, N,4-trimethylaniline exhibited potent inhibitory capability ($IC_{50} = 35.40 \pm 0.82$ μ M). In compounds **36** and **37** the addition of 1-(benzyloxy)-3-methylbenzene and 1-(benzyloxy)-2-methylbenzene groups displayed decline in their inhibitory potential against α -glucosidase with IC_{50} values 49.36 ± 1.20 and 56.72 ± 1.40 μ M respectively. Overall, the different substituents at various positions were involved in the inhibitory capability against α -glucosidase.

The structure-activity relationship (SAR) analysis of dihydropyrimidone derivatives highlights that methoxy substitutions, particularly in para and ortho positions, significantly enhance α -glucosidase inhibitory activity, with compounds like compound **5** with 1,4-dimethoxy-2-methylbenzene ($IC_{50} = 5.30 \pm 0.29$ μ M) showing notable potency. Multi-methoxy configurations, as seen in trimethoxy-substituted compounds, also improve inhibition. Halogenated derivatives (F, Cl, Br) combined with methoxy or hydroxyl groups further increase efficacy, like in compound **11** exemplified by 1-bromo-2,3-dimethoxy-5-methylbenzene ($IC_{50} = 13.14 \pm 0.47$ μ M). In contrast, bulky naphthalene groups decrease activity due to steric hindrance, while electron-withdrawing nitro groups, such as in 1-methyl-4-nitrobenzene, enhanced the inhibitory potential in compound **33** 16.10 ± 0.35 μ M. Acetate substitution markedly reduces activity, suggesting it disrupts effective enzyme interaction. Together, these findings underscore that methoxy and halogen/hydroxyl groups are favorable for inhibition, while bulkier or acetate groups are less effective.

Kinetic study

To reveal the inhibition mechanism of the investigated inhibitors, we selected the most potent inhibitors for their mechanistic study to insight into their inhibition pattern. The kinetic study of compound **4** exhibited mixed type of inhibition with K_i value 5.00 ± 0.016 μ M, while compounds **5** and **13** exhibited a competitive type of inhibition with K_i values, 8.37 ± 0.008 and 3.77 ± 0.002 μ M respectively (Table 2; Fig. 4). In competitive type of inhibition, the compound binds with the active site residue of the enzyme, hence this type of inhibition increases the K_m of enzyme while V_{max} of the enzyme remains constant (Fig. 4D & G). On the other hand, in mixed type of inhibition the inhibitor can bind to the active site or allosteric site of the enzyme. Thus, increase or decrease K_m , depending on the affinity of the inhibitor while V_{max} always decreases due to the binding of inhibitor (Fig. 4A).

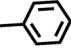
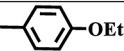
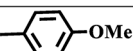
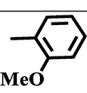
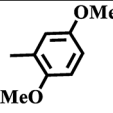
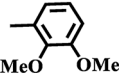
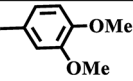
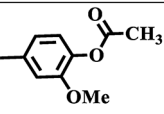
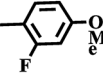
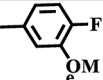
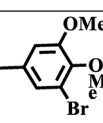
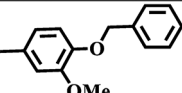
Compound	R	Percent inhibition (0.5mM)	α -Glucosidase inhibitory activity IC ₅₀ \pm SEM (μ M)
1		83.40	31.16 \pm 0.42
2		90.57	9.20 \pm 0.30
3		84.69	10.50 \pm 0.63
4		91.50	7.34 \pm 0.28
5		91.68	5.30 \pm 0.29
6		90.85	8.42 \pm 0.36
7		91.74	11.31 \pm 0.36
8		82.40	37.62 \pm 0.70
9		87.93	15.36 \pm 0.56
10		89.35	17.28 \pm 0.46
11		91.38	13.14 \pm 0.47
12		76.53	34.69 \pm 0.72

Table 1. Inhibitory activities of dihydro pyrimidine derivatives against α -glucosidase (1–37). SEM: Standard Error of the Mean ($n=3$); NA: Not Active.

Cytotoxicity evaluation against BJ cell line

The cytotoxicity evaluation results against the BJ cell line for all tested compounds are presented in Figs. 5, 6, 7, 8 and 9. Specifically, Fig. 5 illustrates the results for compounds 1–7, Fig. 6 for compounds 8–14, Fig. 7 for compounds 15–21, Fig. 8 for compounds 22–28, and Fig. 9 for compounds 29–34. Three different concentrations were used according to their inhibitory potency against α -glucosidase including, 60, 30 and 15 μ M. All compounds exhibited non-cytotoxic effect as at the highest concentration the cell growth percent inhibition is below 25% while at 15 μ M the percent inhibition is below 10%. These significant findings insight into the level of safety of these identified inhibitors. As the non-cytotoxic nature of enzyme inhibitors could

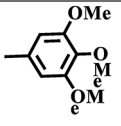

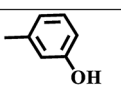
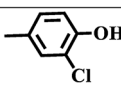
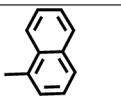
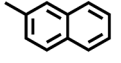


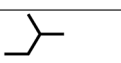
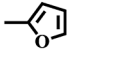
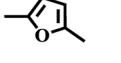

13		90.86	6.14 ± 0.27
14		91.57	18.26 ± 0.51
15		90.13	20.44 ± 0.38
16		90.60	14.30 ± 0.27
17		72.11	44.64 ± 1.10
18		76.80	40.25 ± 0.78
19		34.60	N/A
20		41.27	N/A
21		39.66	N/A
22		75.64	47.30 ± 1.32
23		73.68	50.33 ± .23
24		76.94	46.25 ± 0.65

Table 1. (continued)

be a drug candidate for the pharmaceutical applications. Therefore, these inhibitors could be a possible drug candidate for the treatment of diabetes.

Molecular docking

Herein, the molecular docking simulation was employed to rationalize the observed anti-glucosidase activity. The docking results reveal that the docked compounds accommodated well in the binding site of α -glucosidase located at the C-terminal domain (Fig. 10). Similarly, the compound 2 displayed the lowest docking score of -7.6 kcal/mol followed by 13, 5, 6, 3 and 4 with the docking scores of -7.3, -7.2, -6.7, -6.4 and -5.7 kcal/mol, respectively. Insight into the docked pose of compound 2, reveal the significant hydrogen bond contacts and a network of hydrophobic interactions (Fig. 10A). The oxygen of dihydro pyrimidine scaffold mediates three hydrogen bonds with the side chain of Glu304, Asn347 and Asp349 with a bond distance of 3.2 Å, 2.5 Å and 2.2 Å, respectively. Further, the protein-ligand complex was stabilized a π - π interaction with Phe300 and several hydrophobic interactions with Tyr71, Phe177, Arg212, Thr215, Tyr344, His348 and Gln350. Interestingly, compound 3 exhibited a binding mode similar to that of 2, with the same types of interactions (Fig. 10B). Similarly, the oxygen of dihydro pyrimidine scaffold establishes three hydrogen bonds with the side chain of Glu304, Asn347 and Asp349 with a bond distance of 3.2 Å, 2.4 Å and 2.1 Å, respectively while the pyrimidine ring mediate π - π stacking with Phe300. Moreover, the Tyr71, Phe177, Arg212, Thr215, Tyr344, His348 and Gln350 of α -glucosidase were involved in hydrophobic interactions with the compound. In case of compound 4, slightly different binding was observed (Fig. 10C). The dihydro pyrimidine scaffold bend towards the Tyr71, Arg212 and His348 and moves away from the Phe177, Thr215, Phe300 and Glu304. Further, the oxygen of substitution mediates a hydrogen bond with Asn347 with a bond distance of 2.1 Å. The compound 5 also demonstrated a network of significant interactions with the binding site residues of α -glucosidase (Fig. 10D). The dihydro pyrimidine scaffold sandwich between the Phe177, Phe300 and Asp349 and by mediating hydrophobic interactions while a hydrogen bond was observed with the side chain of Tyr71. Other binding site residues including Arg212, Asn347 and His348 were involved in the hydrophobic interaction with the compound. In case of compound 6 and compound 13, the dihydro pyrimidine scaffold stacked between the Tyr71, Phe177,

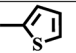
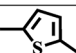
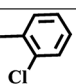
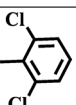
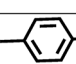
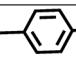
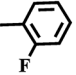
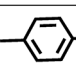
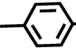
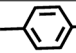
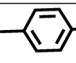
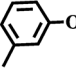
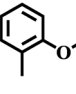
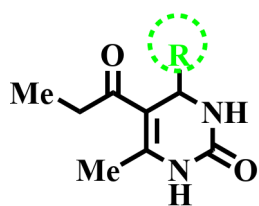
25		77.81	42.90 ± 0.56
26		81.57	39.62 ± 1.11
27		87.74	25.40 ± 0.61
28		88.42	22.61 ± 0.70
29		85.66	27.19 ± 0.46
30		89.26	20.17 ± 0.54
31		84.92	18.33 ± 0.41
32		85.79	26.10 ± 0.56
33		91.36	16.10 ± 0.35
34		74.86	53.19 ± 1.42
35		86.94	35.40 ± 0.82
36		73.28	49.36 ± 1.20
37		75.11	56.72 ± 1.40
Standard*	Acarbose	59.37	873.34 ± 1.67

Table 1. (continued)



Compounds 1-37

Fig. 3. Structure activity relationship of compounds 1–37.

Compound	IC ₅₀ ± (SEM) μM	K _i ± (SEM) μM	Type of inhibition
4	7.34 ± 0.28	5.00 ± 0.016	Competitive
5	5.30 ± 0.29	8.37 ± 0.008	Competitive
13	6.14 ± 0.27	3.77 ± 0.002	Competitive

Table 2. Kinetic study results.

Thr215 and Phe300 and mediates the hydrophobic interactions (Fig. 10E,F). While the substitution on the dihydro pyrimidine scaffold exhibited hydrophobic interactions with the Tyr344, His348, Asn347 and Asp349 of α -glucosidase. In addition, the compound **6** also displayed a hydrogen bond with side chain of Asn347 with a bond distance of 3.3 Å. Overall the results indicated that the different substitutions alter the interactions within the active site, potentially impacting their inhibitory effectiveness.

Molecular dynamics simulation

The molecular dynamics (MD) simulation of three of the most potent compounds (**4**, **5** and **13**) with α -glucosidase was carried out to evaluate the time dependant behaviour of the complexes. The compound **4** with the α -glucosidase enzyme revealed a stable interaction between the ligand and protein throughout the simulation period. The protein-ligand RMSD plot showed that the C α atoms of the protein stabilize around 2.5 Å after an initial equilibration phase, which indicated that the enzyme reached a steady conformation (Fig. 11). The ligand RMSD remained fairly constant around 3.0 Å, which suggested that compound **4** maintain a stable binding position within the binding site of the enzyme. Analysis of protein RMSF highlighted the flexibility of individual residues, with most residues showing low fluctuations (approximately 1 Å), which also indicated stability (Fig. 11). However, certain regions, particularly between residues 250–300 and near the C-terminal end, exhibited higher flexibility, likely due to the presence of loops or solvent-exposed regions. The protein-ligand contact profile revealed significant interactions, with key residues like Asp68, Thr125, Glu214, Arg212, and Asp349 showing strong hydrogen bonding and hydrophobic interactions (Fig. 11). Principal Component Analysis (PCA) further demonstrated that the complex explores distinct conformational states, with clusters indicating stable conformations that the system adopts during the simulation (Fig. 11).

The MD simulation of compound **5** with the α -glucosidase enzyme revealed a stable and well-defined interaction within the enzyme's binding site. The protein-ligand RMSD plot showed that the C α atoms of the protein stabilize around 2.8 Å after the initial equilibration phase, which indicated that the protein reached a consistent conformation (Fig. 12). The ligand RMSD remains relatively steady around 2.5–3.0 Å, which suggested that compound **5** maintains a stable position within the binding site throughout the simulation. The protein RMSF analysis revealed low flexibility across most residues, with slight fluctuations observed primarily in the region between residues 300 and 400 (Fig. 12). In terms of protein-ligand contacts, key residues such as Asp69, Arg212, Asp349, and Asp408 were frequently involved in hydrogen bonding, hydrophobic, and ionic interactions, which highlighted their importance in maintaining the binding stability of compound **5** within the binding site (Fig. 12). The PCA plot further demonstrated that the complex samples distinct conformational states, with clustering patterns which suggested the system transitions between specific substates while remaining within stable conformational regions (Fig. 12).

The MD simulation results for compound **13** with the α -glucosidase enzyme indicated a stable interaction pattern throughout the simulation. The protein-ligand RMSD plot showed that the C α atoms of the protein reach a steady RMSD around 3.5 Å after an initial increase, which suggested that the protein's conformation stabilizes over time (Fig. 13). The ligand RMSD rises slightly higher, stabilizing around 6–7 Å, which suggested that while compound **13** remains bound, it may exhibit some flexibility within the binding site. The protein RMSF analysis revealed notable fluctuations in certain residue regions, especially around residues 200–300 and 500–550, potentially indicating flexible regions (Fig. 13). The protein-ligand contacts plot highlighted that residues like Asp69, Met71, and Arg143 play key roles in stabilizing the ligand, and showed significant interactions such as hydrogen bonds, hydrophobic contacts, and water bridges (Fig. 13). Additionally, the PCA plot suggested that the system explores multiple conformational states but remains within a stable conformational space, with transitions indicated by color gradients across frames (Fig. 13).

Binding free energy

The binding free energy for compounds **4**, **5**, and **13** with α -glucosidase enzyme, was calculated using the Prime MM-GBSA module in Schrödinger (Fig. 14). Compound **4** showed a binding energy (ΔG_{Bind}) of -23.13 kcal/mol, with a substantial coulombic interaction ($\Delta G_{\text{Coulomb}} = -20.50$ kcal/mol) and favourable van der Waals interactions ($\Delta G_{\text{vdW}} = -31.34$ kcal/mol). The lipophilic ($\Delta G_{\text{Lipo}} = -6.42$ kcal/mol) and hydrogen bonding ($\Delta G_{\text{Hbond}} = -2.76$ kcal/mol) terms also contributed to the stability of binding. The solvent energy ($\Delta G_{\text{Solv}} = 36.30$ kcal/mol) opposes binding but was counterbalanced by other interactions. The ligand strain energy was 2.29 kcal/mol. Compound **5** had a binding energy of -20.67 kcal/mol, with a smaller coulombic contribution ($\Delta G_{\text{Coulomb}} = -4.58$ kcal/mol) but a stronger lipophilic interaction ($\Delta G_{\text{Lipo}} = -12.31$ kcal/mol). The van der Waals interactions ($\Delta G_{\text{vdW}} = -34.94$ kcal/mol) significantly supported binding stability. The solvent energy ($\Delta G_{\text{Solv}} = 31.79$ kcal/mol) partly opposes binding, while the ligand strain energy was 1.36 kcal/mol. Compound **13** exhibited the strongest binding affinity with a ΔG_{Bind} of -30.15 kcal/mol. Despite a minimal coulombic contribution ($\Delta G_{\text{Coulomb}} = -0.37$ kcal/mol), the van der Waals interactions ($\Delta G_{\text{vdW}} = -37.87$ kcal/mol) and

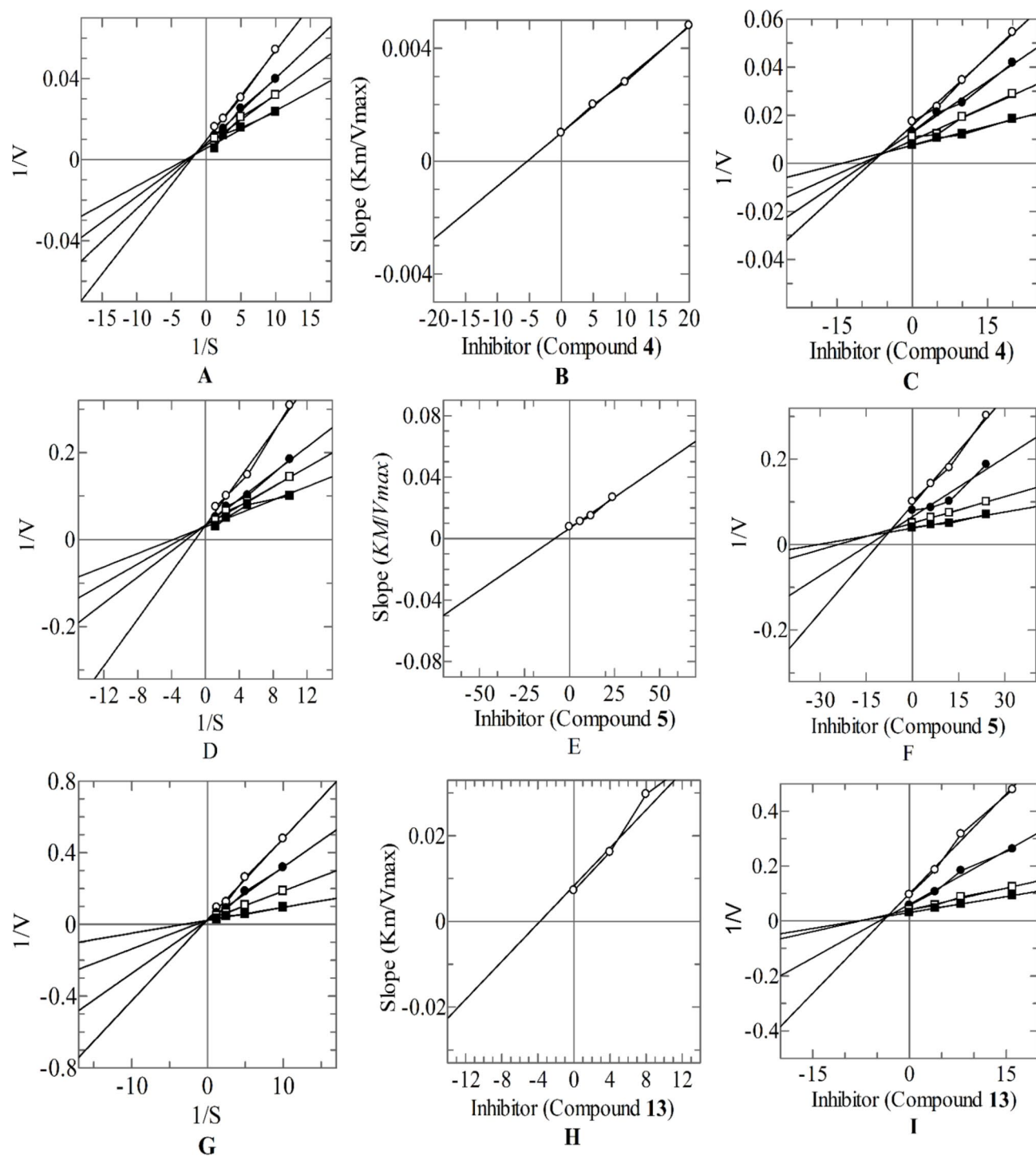


Fig. 4. Mode of inhibition of α -glucosidase by compound 4, 5 and 13 (A,D,G) Lineweaver-Burk plot of reciprocal of rate of reaction (V) vs. reciprocal of substrate in the absence of (filled rectangle), and in the presence of 16.00 μ M (open circle), 8.00 μ M (filled circle), and 4.00 μ M (open rectangle), of compound 4, 5 and 13. (B,E,H) Secondary replot of Line Weaver-Burk plot between the slopes of each line on Line Weaver-Burk plot vs. different concentrations of compound 4, 5 and 13. (C,F,I) Dixon plot of reciprocal of rate of reaction (V) vs. different concentrations of compound 4, 5 and 13.

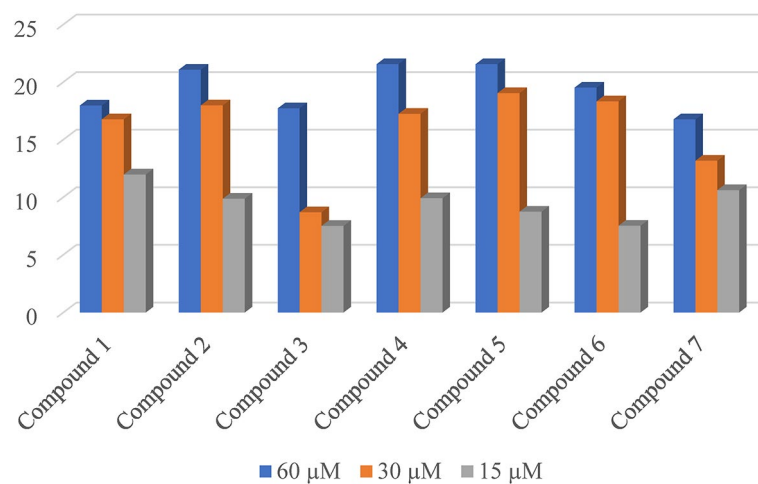


Fig. 5. Cytotoxicity evaluation results against BJ cell line of compounds 1–7.

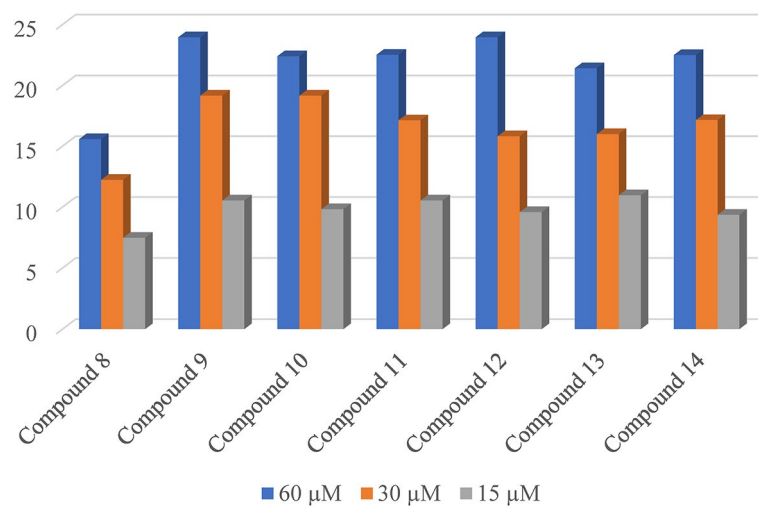


Fig. 6. Cytotoxicity evaluation results against BJ cell line of compounds 8–14.

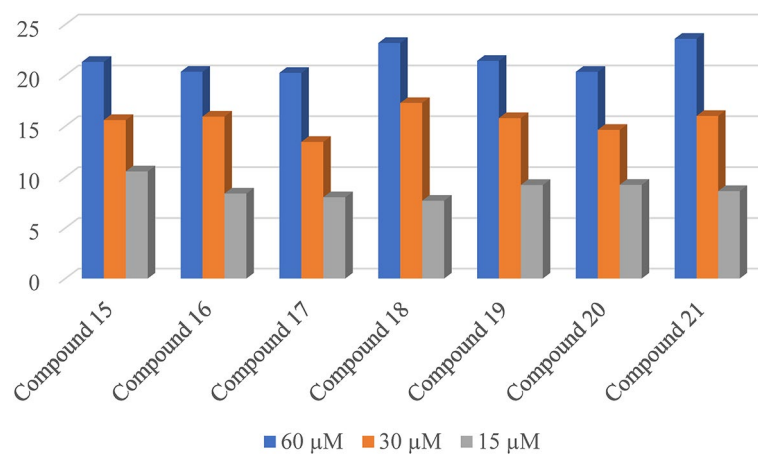


Fig. 7. Cytotoxicity evaluation results against BJ cell line of compounds 15–21.

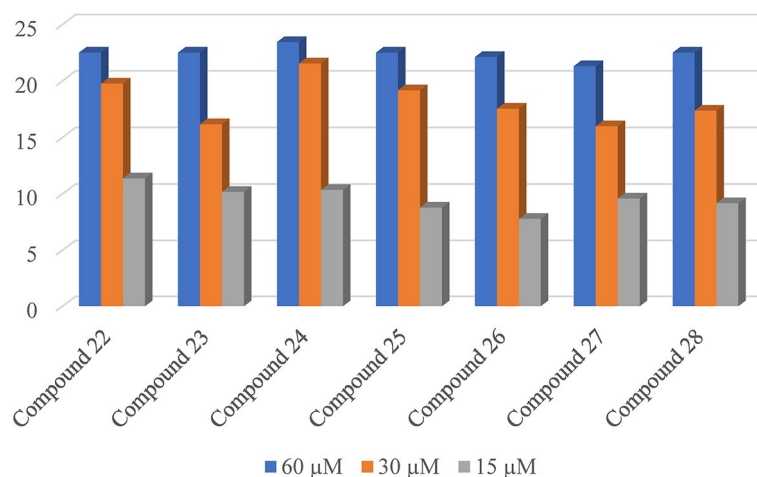


Fig. 8. Cytotoxicity evaluation results against BJ cell line of compounds 22–28.

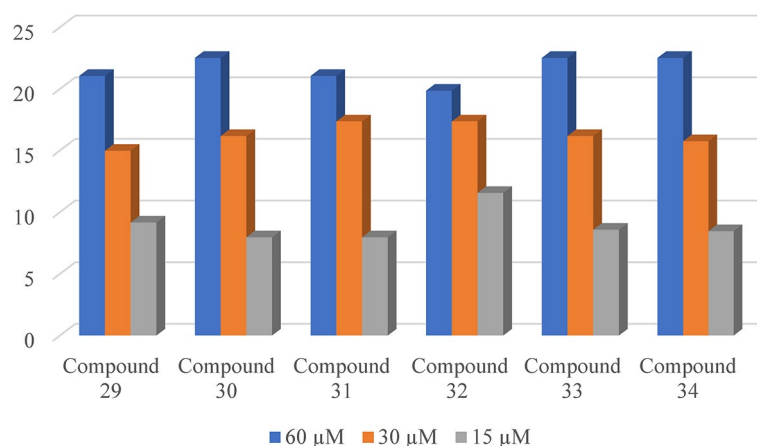


Fig. 9. Cytotoxicity evaluation results against BJ cell line of compounds 29–34.

lipophilic effect ($\Delta G_{\text{Lipo}} = -12.00$ kcal/mol) were highly favourable, which compensate the opposing solvent energy ($\Delta G_{\text{Solv}} = 20.43$ kcal/mol). The ligand strain energy was 2.01 kcal/mol.

Discussion

The dihydropyrimidone derivatives demonstrated promising α -glucosidase inhibitory activity, with compounds 4, 5, and 13 identified as potent competitive inhibitors based on kinetic studies. These compounds increased the K_m without affecting V_{max} , confirming competitive inhibition, where the inhibitor binds at the enzyme's active site. Cytotoxicity evaluation on BJ cell lines indicated that all active compounds-maintained cell viability, with less than 25% inhibition even at 60 μ M, confirming their non-cytotoxic nature and suitability as drug candidates. The results of MD simulations also indicate that all compounds maintain stable binding interactions throughout the simulations, with favourable contributions from key interactions that support their binding affinity. Notably, the binding free energies of compounds 13, 4, and 5 show a clear correlation with their inhibition constants values, demonstrating that compounds with more negative ΔG_{Bind} have stronger binding affinities, as reflected in lower K_i values. Compound 13, with the most favourable binding energy of -30.15 kcal/mol, exhibited the strongest binding affinity, correlating with its lowest K_i value of 3.77 ± 0.002 μ M. Compound 4, with a binding energy of -23.13 kcal/mol, also showed a moderate binding affinity, reflected in a K_i of 5.00 ± 0.016 μ M. In contrast, compound 5 had the least favourable binding energy of -20.67 kcal/mol, which corresponds with its highest K_i value of 8.37 ± 0.008 μ M. These findings highlight the safety and efficacy of these competitive α -glucosidase inhibitors, underscoring their potential for therapeutic development in diabetes management.

Experimental Chemistry

We bought reagents from Sigma-Aldrich in the USA. Analytical grade materials were used for all reagents and solvents throughout. On pre-coated silica gel, GF-254, thin layer chromatography was carried out (Merck,

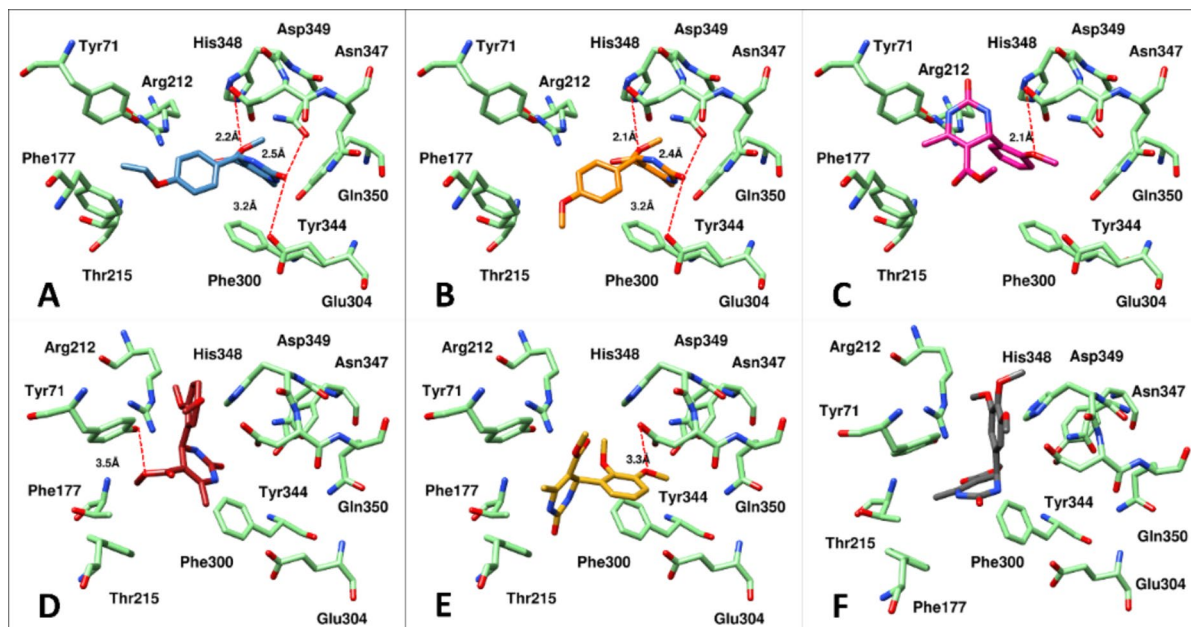


Fig. 10. Molecular interactions between the six most potent compounds and the α -glucosidase. The residues lining the binding site of α -glucosidase are displayed in lime green sticks. A–E) The compounds 3–6 and F) compound 13 are displayed in different colour sticks. The red dotted lines represented the hydrogen bond contacts.

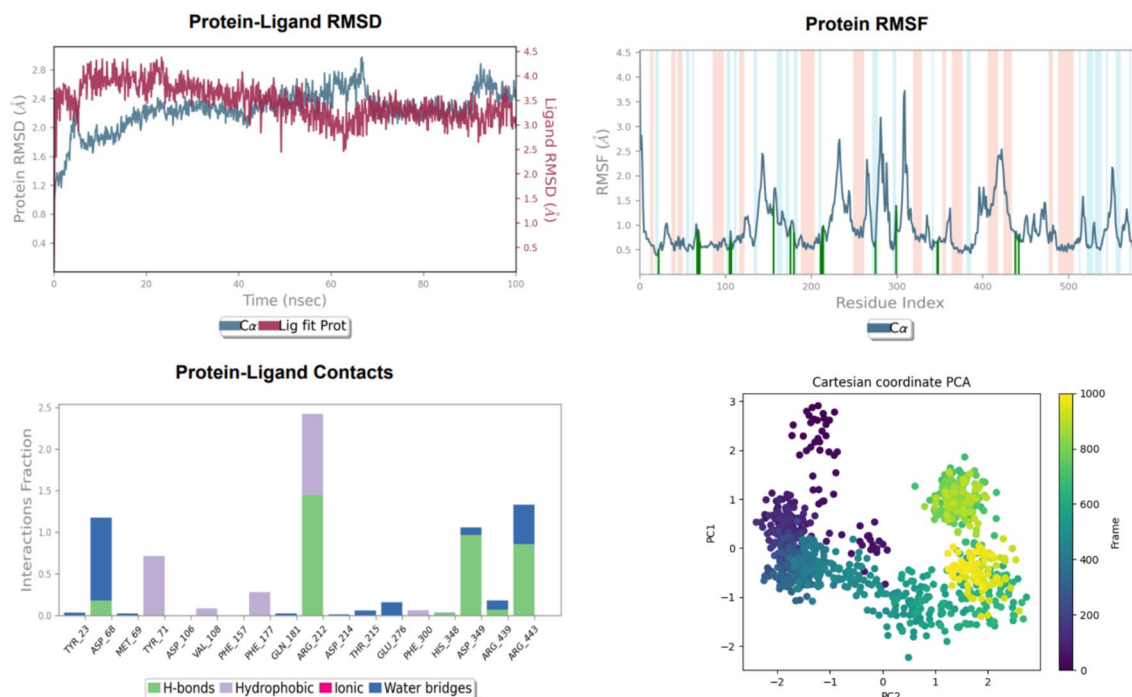


Fig. 11. MD simulation results of compound 4 with α -glucosidase enzyme. Protein-Ligand RMSD and RMSF show the stability and flexibility of the complex, while Protein-Ligand Contacts identified the key residues involved in binding. PCA analysis indicated a stable conformational space for the complex.

Germany). At 254 and 366 nm, ultraviolet light was used to see the spots. The compounds' melting points were calculated using a BUCHI-M560 melting point equipment. Mass spectrometers MAT 312 and MAT 113D were used to record the spectra. On a Bruker AM spectrometer that operated at 300, 400, and 500 MHz, the $^3\text{H}^1$, C-NMR data were collected. The coupling constant (J) is given in Hz, and the chemical shift values are given in ppm (δ), relative to tetramethyl silane (TMS) as an internal reference.

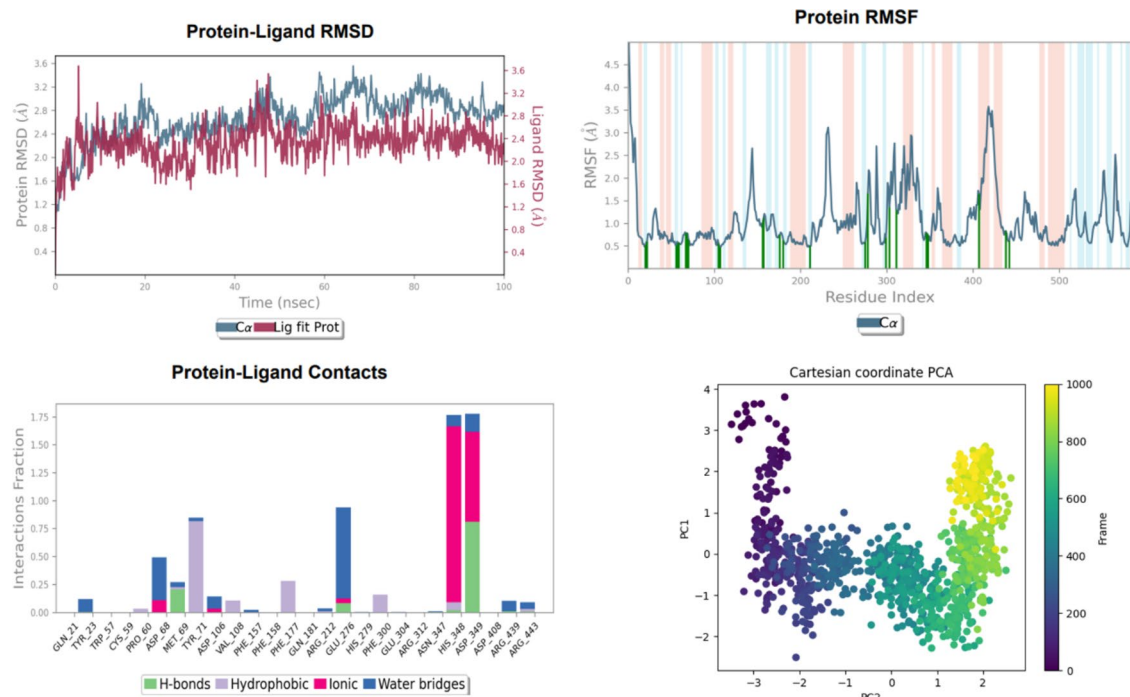


Fig. 12. MD simulation results of compound **5** with α -glucosidase enzyme. RMSD and RMSF analysis revealed stable binding and moderate flexibility. Protein-Ligand Contacts highlighted essential interactions, and PCA showed the complex maintaining stability with minor conformational changes.

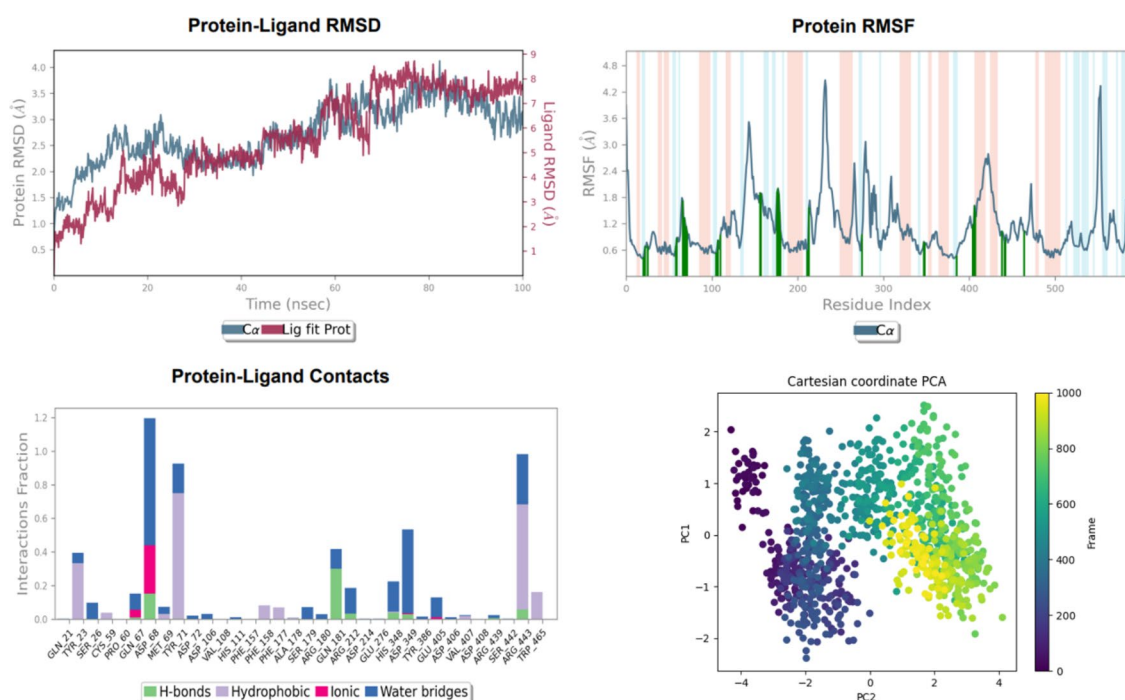


Fig. 13. MD simulation results of compound **13** with α -glucosidase enzyme. RMSD and RMSF plots indicated stable binding with slight ligand flexibility, while Protein-Ligand Contacts identified critical residues in binding stability. PCA revealed the complex exploring a stable conformational space.

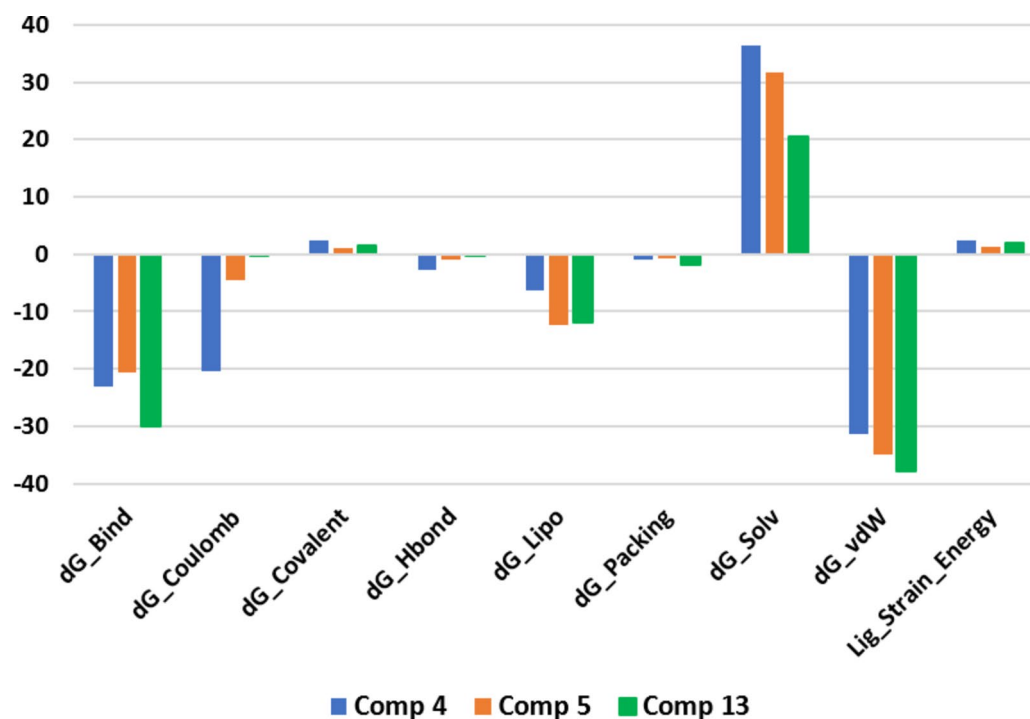


Fig. 14. Binding free energy results for compounds 4, 5, and 13 with the α -glucosidase enzyme, calculated using the Prime MM-GBSA module in Schrödinger. The contributions of various energy terms, including Coulombic, van der Waals, lipophilic, hydrogen bonding, and solvent energies, to the overall binding affinity are depicted.

General experimental procedures

In a 100 mL round-bottomed flask, the following ingredients were added: urea (1 mmol), ethyl acetoacetate (1.2 mmol), substituted aryl aldehyde (1 mmol), and copper nitrate trihydrate (10 mol percent) as catalyst. The mixture was heated at 80–90 °C while being stirred continuously. The reaction's success was periodically monitored using TLC. After the reaction was finished, the solid mixture was washed with extra distilled water and then recrystallized from ethanol to produce pure products in large yields²⁴.

In vitro α -glucosidase inhibitory assay

Assay was carried out using our already available methodology⁴⁰. The experiment was performed by employing 20 μ L of each test compound in various concentrations were plated in triplicate, 135 μ L of 0.5 mM Phosphate buffer was added followed by 20 μ L of enzyme solution. Plate was incubated at 37 °C for 15 min and readings were recorded at 400 nm. After 15 min of incubation, 25 μ L of substrate solution was added and changes in absorbance was recorded for 30 min at 400 nm. Final absorbance was taken at the end of 30 min. Blank and standard inhibitors were also implemented in each experiment. (7% DMSO) was used as negative control, while acarbose was used as positive control.

Kinetic study assay

To assess the mechanism of action of the α -glucosidase the similar procedure was followed with a slight modification. Here, in the enzyme kinetic experiments we employed four different concentrations of the substrate after 15 min incubation at 37 °C. By the same way we dissolved the substrate in the same 50 mM phosphate buffer and after 15 min incubation four different concentration 0.1, 0.2, 0.4 and 0.8 mM was added to initiate the reaction, and experiment was run for 30 min and changes in absorbance was recorded at 400 nm.

Cytotoxicity effect evaluation of compounds 1–37

We used the BJ cell line to conduct in-vitro research of all the tested compounds except non-active compounds 19–21 to examine the cytotoxic effect of these inhibitors. Here, we planned our experiment to use a precise number of cells 6×10^4 cells/well into the plate. We filled each well with 100 μ L, and then we incubated it for 24 h at 37 °C in 5% CO₂. Subsequently, the 96-well plate was incubated for 48 h under identical precise experimental conditions with 50 μ L/well (60, 30 and 15 μ M) of the investigated drugs plus 150 μ L/well of fresh medium. Following the second incubation cycle, 200 μ L of yellow MTT dye was added to each well in a 1:10 ratio to replace the old media, and the mixture was incubated for four hours. Subsequently, the dye was eliminated, and 100 μ L/well of DMSO (dimethyl sulfoxide) cell culture grade was added to the 96-well plate to dissolve the formazan crystals of MTT dye that had turned purple. Using a spectrophotometer, the resulting variations in the (OD) optical density were tracked at 540 at the conclusion of the experiment.

Statistical analysis

The programs were employed to analyze the attained results for biological activity, the SoftMax Pro package and Excel were utilized.

The given formula below was used to calculate percent inhibition.

$$\%Inhibition = 100 - \left(\frac{O.D_{test\ compound}}{O.D_{control}} \right) \times 100 \quad (1)$$

EZ-FIT (Perrella Scientific, Inc., USA) was used for IC_{50} calculations of all tested samples. To overcome on the expected errors all experiments were performed in triplicate, and variations in the results are reported in Standard Error of Mean values (SEM).

$$SE = \frac{\sigma}{\sqrt{n}} \quad (2)$$

Molecular docking

Molecular docking is a computational technique used in drug design to predict the preferred binding orientation and interaction strength between a small molecule and a target protein, aiding in the identification of potential therapeutic compounds^{41,42}. Herein, the docking studies were carried out to predict the molecular interactions of the synthesized compounds with α -glucosidase enzyme. The selected compounds with the most potent activity including 3–6 and 13 were sketched in MOE v.2019.01 software⁴³. Afterwards, the compounds were subjected to structure correction and protonation followed by energy minimization using the MMFF94x force field. Since the crystal structure of α -glucosidase (*Saccharomyces cerevisiae*) is not reported yet, we generated the homology model using the isomaltase from *Saccharomyces cerevisiae* (PDB ID 3A4A) as a template⁴⁴. The geometry of the generated model was corrected using the Structure Correction module of MOE. Subsequently, the protons were added, and partial charges were applied. The structure was then subjected to energy minimization using the Amber10:EHT force field. Previously established protocol was used for docking studies^{45–47}. Briefly, Triangular Matcher was used as a placement method with Rigid protocol while London dG and GBVI/WSA dG were kept as scoring and rescoring functions. For each compound, thirty poses were generated and five best were retained for analysis. All the graphics were rendered by Chimera software⁴⁸.

Molecular dynamics simulation

Molecular dynamics (MD) simulations were performed using Desmond on a Linux machine⁴⁹. Protein structures were prepared using the Protein Preparation Wizard in Schrödinger. System preparation for MD simulations was carried out with the System Builder module in Desmond, employing the TIP3P water model to solvate each protein within an orthorhombic box with a 10 Å buffer. Na⁺ ions were introduced to neutralize the system, and a NaCl concentration of 0.15 M was simulated to mimic physiological conditions. Before running the production MD simulations, each system was equilibrated using Desmond's default relaxation protocol, which includes two stages of energy minimization (with and without restraints) followed by four stages of MD simulations with progressively decreasing restraints under the NVT/NPT ensembles. The production MD simulations were then conducted for 100 ns under the NPT ensemble using the OPLS3e force field. Finally, the resulting trajectories were analyzed using the Simulation Event Analysis tool in Desmond to extract key dynamic properties and interactions.

Binding free energy

To evaluate the binding free energy of each compound with the α -glucosidase enzyme, we employed Molecular Mechanics-Generalized Born Surface Area (MM-GBSA) calculations using Schrödinger's Prime module. MM-GBSA is a thermodynamic approach widely recognized for its effectiveness in assessing binding affinities⁵⁰. This method calculates the binding free energy (ΔG_{bind}) based on the optimized energies of the free ligand, free receptor, and ligand-receptor complex. For our analysis, the Prime MM-GBSA tool was used to predict the energy of optimized free ligands, free receptor (α -glucosidase), and the resulting ligand-receptor complex. These calculations were performed in an implicit solvent environment generated using the VSGB solvation model within the S-OPLS force field.

Conclusion

The present study was designed to investigate new inhibitors against the key metabolic enzyme of carbohydrate α -glucosidase to develop a therapeutic approach for the treatment of diabetes type 2. In conclusion, this study identifies thirty-four potent α -glucosidase inhibitors with IC_{50} values ranging from 20.47 to 86.36 μ M, demonstrating superior inhibitory potency compared to the standard drug acarbose ($IC_{50} = 875.75 \pm 2.10 \mu$ M). The most potent compound, inhibitor 5, displayed a competitive inhibition mechanism, engaging directly with the active site of α -glucosidase, as confirmed by kinetic studies and molecular docking analysis. The docking and MD simulation results further support that these inhibitors effectively occupy the enzyme's binding site, preventing substrate access. Additionally, cytotoxicity assays on BJ cell lines confirmed that all compounds were non-cytotoxic, reinforcing their potential safety profile. These findings suggest that the identified inhibitors are promising candidates for further development in diabetes type 2 treatment, warranting additional studies to fully explore their medicinal properties and therapeutic efficacy.

Data availability

The datasets used and/or analysed during the current study available from the corresponding author on reasonable request.

Received: 19 September 2024; Accepted: 9 December 2024

Published online: 30 December 2024

References

- Rathmann, W. & Giani, G. Global prevalence of diabetes: estimates for the year 2000 and projections for 2030. *Diabetes Care*. **27**, 2568–2569 (2004).
- Bonora, E. & Muggeo, M. Postprandial blood glucose as a risk factor for cardiovascular disease in Type II diabetes: the epidemiological evidence. *Diabetologia* **44**, 2107–2114 (2001).
- Hogan, P., Dall, T., Nikolov, P. & American Diabetes Association. Economic costs of diabetes in the US in 2002. *Diabetes Care* **26**, 917–932 (2003).
- Koro, C. E., Lee, B. H. & Bowlin, S. J. Antidiabetic medication use and prevalence of chronic kidney disease among patients with type 2 diabetes mellitus in the United States. *Clin. Ther.* **31**, 2608–2617 (2009).
- Bailey, C. J. Drugs on the horizon for diabetes. *Curr. Diab Rep.* **5**, 353–359 (2005).
- Krentz, A. J., Patel, M. B. & Bailey, C. J. New drugs for type 2 diabetes mellitus: what is their place in therapy? *Drugs* **68**, 2131–2162 (2008).
- Krentz, A. J. & Bailey, C. J. Oral antidiabetic agents: current role in type 2 diabetes mellitus. *Drugs* **65**, 385–411 (2005).
- Sarabu, R. et al. Recent advances in therapeutic approaches to type 2 diabetes. In *Annual Reports in Medicinal Chemistry* (eds. Doherty, A. M.) Vol. 40 167–181 (Academic Press, 2005).
- Tilley, J., Grimsby, J., Erickson, S. & Berthel, S. Diabetes Drugs: Present and Emerging. In *Burger's Medicinal Chemistry and Drug Discovery* 1–38 (Wiley, 2010). <https://doi.org/10.1002/0471266949.bmc198>.
- Levetan, C. Oral antidiabetic agents in type 2 diabetes. *Curr. Med. Res. Opin.* **23**, 945–952 (2007).
- Ullah, S. et al. 2-Mercapto benzothiazole derivatives: As potential leads for the diabetic management. *Med. Chem.* **16**, 826–840 (2020).
- Akhter, S. et al. Synthesis, crystal structure and Hirshfeld Surface analysis of benzamide derivatives of thiourea as potent inhibitors of α -glucosidase *in-vitro*. *Bioorg. Chem.* **107**, 104531 (2021).
- Avci, D. et al. Three novel Cu(II), Cd(II) and Cr(III) complexes of 6-Methylpyridine-2-carboxylic acid with thiocyanate: Synthesis, crystal structures, DFT calculations, molecular docking and α -Glucosidase inhibition studies. *Tetrahedron* **74**, 7198–7208 (2018).
- Kausar, N. et al. Celebrex derivatives: Synthesis, α -glucosidase inhibition, crystal structures and molecular docking studies. *Bioorg. Chem.* **106**, 104499 (2021).
- Becan, L. & Wójcicka, A. Synthesis, anti-hepatitis B and C virus activity & and antitumor screening of novel thiazolo[4,5-D]-pyrimidine derivatives. *Acta Pol. Pharm.* **73**, 107–114 (2016).
- Kindon, N. et al. From UTP to AR-C118925, the discovery of a potent non nucleotide antagonist of the P2Y2 receptor. *Bioorg. Med. Chem. Lett.* **27**, 4849–4853 (2017).
- Kamat, V. et al. In vitro α -amylase and α -glucosidase inhibition study of dihydropyrimidinones synthesized via one-pot Biginelli reaction in the presence of a green catalyst. *Bioorg. Chem.* **143**, 107085 (2024).
- Abdel-Galil, E., Moawad, E. B., El-Mekabaty, A. & Said, G. E. Synthesis, characterization and antibacterial activity of some new thiazole and thiazolidinone derivatives containing phenyl benzoate moiety. *Synth. Commun.* **48**, 2083–2092 (2018).
- Kendre, B., Bhusare, S. & Hardas, P. Antimicrobial and anti-inflammatory activity studies of novel thiazolopyrimidines. *Am. J. PharmTech Res.* **10**, 55–73 (2020).
- Fatima, S. et al. One pot efficient diversity oriented synthesis of polyfunctional styryl thiazolopyrimidines and their bio-evaluation as antimalarial and anti-HIV agents. *Eur. J. Med. Chem.* **55**, 195–204 (2012).
- Cai, D. et al. Synthesis of some new thiazolo[3,2-a]pyrimidine derivatives and screening of their in vitro antibacterial and antitubercular activities. *Med. Chem. Res.* **25**, 292–302 (2016).
- Kumar, S., Deep, A. & Narasimhan, B. A. Review on synthesis, anticancer and antiviral potentials of pyrimidine derivatives. *Curr. Bioact. Compd.* **15**, 289–303.
- Kumar, A. et al. Dihydropyrimidinone scaffold and potential therapeutic targets 67–101. <https://doi.org/10.1016/B978-0-443-19094-0.00004-7> (2023).
- Ali, F. et al. Dihydropyrimidinones: As novel class of β -glucuronidase inhibitors. *Bioorg. Med. Chem.* **24**, 3624–3635 (2016).
- Yadav, K. P. et al. Synthesis and biological activities of benzothiazole derivatives: A review. *Intell. Pharm.* **1**, 122–132 (2023).
- Ahmadi, A. et al. Synthesis and evaluation of the hypoglycemic and hypolipidemic activity of sulfonamide-benzothiazole derivatives of benzylidene-2,4-thiazolidinedione. *Mini Rev. Med. Chem.* **17**, 721–726 (2017).
- Meltzer-Mats, E. et al. Synthesis and mechanism of hypoglycemic activity of benzothiazole derivatives. *J. Med. Chem.* **56**, 5335–5350 (2013).
- Ilyas, U. et al. Investigation of anti-diabetic potential and molecular simulation studies of dihydropyrimidinone derivatives. *Front. Endocrinol. (Lausanne)*. **13**, 1022623 (2022).
- Yar, M. et al. Novel synthesis of dihydropyrimidines for α -glucosidase inhibition to treat type 2 diabetes: in vitro biological evaluation and in silico docking. *Bioorg. Chem.* **54**, 96–104 (2014).
- Fadhel, A., Albaayit, S., Maharjan, R. & Abdullah, R. Hezmee Mohd Noor, M. Evaluation of anti-methicillin-resistant *Staphylococcus aureus* property of zerumbone. *J. Appl. Biomed.* <https://doi.org/10.32725/jab.2022.002> (2022).
- Albaayit, S. F. A., Abdullah, R. & Noor, M. H. M. Zerumbone-loaded nanostructured lipid carrier gel enhances wound healing in diabetic rats. *BioMed Res. Int.* 1129297 (2022).
- Albaayit, S. F. A., Maharjan, R. & Khan, M. Evaluation of hemolysis activity of zerumbone on RBCs and brine shrimp toxicity. *Baghdad Sci. J.* **18**, 0065–0065 (2021).
- Albaayit, S. F. A., Khan, M. & Abdullah, R. Zerumbone induces growth inhibition of Burkitt's lymphoma cell line via apoptosis. *Nat. Volatiles Essent. Oils* **8**, 56–63 (2021).
- Albaayit, A. & Fadhel, S. Enzyme inhibitory and anti-cancer properties of *Moringa peregrina*. *Vitae (Medellin)* **1**, 7 (2024).
- Reddy, S. Synthesis and cytotoxic evaluation for some new dihydropyrimidinone derivatives for anticancer activity. *Lett. Drug Des. Discov.* **10**, 699–705 (2013).
- Abd El-Aleam, R. H., George, R. F., Hassan, G. S. & Abdel-Rahman, H. M. Synthesis of 1,2,4-triazolo[1,5-a]pyrimidine derivatives: Antimicrobial activity, DNA Gyrase inhibition and molecular docking. *Bioorg. Chem.* **94**, 103411 (2020).
- Zhang, X. et al. Design, synthesis and anti-tumor evaluation of 1,2,4-triazol-3-one derivatives and pyridazinone derivatives as novel CXCR2 antagonists. *Eur. J. Med. Chem.* **226**, 113812 (2021).
- Omar, A. M. et al. New pyrimidines and triazolopyrimidines as antiproliferative and antioxidants with cyclooxygenase-1/2 inhibitory potential. *Future Med. Chem.* **11**, 1583–1603 (2019).

39. Bassyouni, F. et al. Promising antidiabetic and antimicrobial agents based on fused pyrimidine derivatives: molecular modeling and biological evaluation with histopathological Effect. *Molecules* **26**, 2370 (2021).
40. Mehreen, S. et al. Phenoxy pendant isatins as potent α -glucosidase inhibitors: reciprocal carbonyl...carbonyl interactions, antiparallel π ... π stacking driven solid state self-assembly and biological evaluation. *RSC Adv.* **12**, 20919–20928 (2022).
41. Shahab, M., Khan, A., Khan, S. A. & Zheng, G. Unraveling the mechanisms of Sofosbuvir resistance in HCV NS3/4A protease: Structural and molecular simulation-based insights. *Int. J. Biol. Macromol.* **267**, 131629 (2024).
42. Suleman, M. et al. Molecular screening of phytochemicals targeting the interface between influenza A NS1 and TRIM25 to enhance host immune responses. *J. Infect. Public Health* **17**, 102448 (2024).
43. Khan, A. et al. Identification of IL-2 inducible tyrosine kinase inhibitors by quantum mechanics and ligand based virtual screening approaches. *J. Biomol. Struct. Dyn.* **42**, 3630–3640 (2024).
44. Yamamoto, K., Miyake, H., Kusunoki, M. & Osaki, S. Crystal structures of isomaltase from *Saccharomyces cerevisiae* and in complex with its competitive inhibitor maltose. *FEBS J.* **277**, 4205–4214 (2010).
45. Ullah, S. et al. Exploring bi-carbazole-linked triazoles as inhibitors of prolyl endo peptidase via integrated in vitro and in silico study. *Sci. Rep.* **14**, 7675 (2024).
46. Ata, A. et al. Identification of potential urease inhibitors and antioxidants based on saccharin derived analogs: Synthesis, *in vitro*, and *in silico* studies. *J. Mol. Struct.* **1274**, 134376 (2023).
47. Muhammad, A. et al. Effects of long-term *Ailanthus altissima* extract supplementation on fear, cognition and brain antioxidant levels. *Saudi Pharm. J.* **31**, 191–206 (2023).
48. Goddard, T. D., Huang, C. C. & Ferrin, T. E. Software extensions to UCSF chimera for interactive visualization of large molecular assemblies. *Structure* **13**, 473–482 (2005).
49. Bowers, K. J. et al. Scalable algorithms for molecular dynamics simulations on commodity clusters. In *SC '06: Proceedings of the ACM/IEEE Conference on Supercomputing* 43. <https://doi.org/10.1109/SC.2006.54> (2006).
50. Wang, E. et al. End-point binding free energy calculation with MM/PBSA and MM/GBSA: Strategies and applications in drug design. *Chem. Rev.* **119**, 9478–9508 (2019).

Acknowledgements

The authors are grateful to the Scientific Research Deanship at King Khalid University, Abha, Saudi Arabia for their financial support through the Small Research Group Project under grant number (RGP.1/149/45).

Author contributions

Conceptualization, F.M., F.A., A.A. and S.U.; Formal analysis, S.A.A., A.D., M.S. and F.A.; Funding acquisition, S.P.A.; Methodology, F.M. and S.U.; Validation, S.A.A., F.A., H.A., R.G. and S.A.; Writing – original draft, F.M. and S.U.; Writing – review & editing, S.P.A., S.A.A., J.U. and S.A. All authors reviewed the manuscript.

Declarations

Competing interests

The authors declare no competing interests.

Additional information

Correspondence and requests for materials should be addressed to S.F.A.A., S.A. or S.U.

Reprints and permissions information is available at www.nature.com/reprints.

Publisher's note Springer Nature remains neutral with regard to jurisdictional claims in published maps and institutional affiliations.

Open Access This article is licensed under a Creative Commons Attribution-NonCommercial-NoDerivatives 4.0 International License, which permits any non-commercial use, sharing, distribution and reproduction in any medium or format, as long as you give appropriate credit to the original author(s) and the source, provide a link to the Creative Commons licence, and indicate if you modified the licensed material. You do not have permission under this licence to share adapted material derived from this article or parts of it. The images or other third party material in this article are included in the article's Creative Commons licence, unless indicated otherwise in a credit line to the material. If material is not included in the article's Creative Commons licence and your intended use is not permitted by statutory regulation or exceeds the permitted use, you will need to obtain permission directly from the copyright holder. To view a copy of this licence, visit <http://creativecommons.org/licenses/by-nc-nd/4.0/>.

© The Author(s) 2024, corrected publication 2025